IET Journals

IET Communications

ISSN 1751-8628

Secure and reliable transmission mechanism for orthogonal frequency-division multiple access worldwide interoperability for microwave access systems

J. Chen[1]   C.-C. Wang[2]

[1]Department of Computer Science and Information Engineering, Chang Gung University, Kweishan, Taoyuan, Taiwan
[2]Department of Electrical Engineering, Chang Gung University, Kweishan, Taoyuan, Taiwan
E-mail: jhchen@mail.cgu.edu.tw

Abstract: The most challenging technical issue in worldwide interoperability for microwave access (WiMAX) networks is to find a way to counteract the interference as well as to solve the fading problem in transmissions. Although IEEE 802.16e standard proposes several mechanisms to handle this difficult problem, there are still many external interferences that may collapse ongoing transmissions. To tackle this thorny problem, the authors develop a method called fault-tolerant transmission mechanism (FTM), which re-permutes and scatters slots in each frame space of the downlink transmission in the medium access control (MAC) layer to achieve a higher probability of success in transmissions. FTM can produce approximately 30% more throughput than the IEEE 802.16 standard can and significantly raise the successful transmission probability, while having each transmitted burst size limited to no more than 20 slots (5% of the total downlink frame space). Therefore by adjusting the burst size, rearranging slot places and comparing their patterns, FTM can provide a more reliable, more secure and more efficient transmission mechanism than IEEE 802.16e transmission mechanism. In addition, it is fully compatible with orthogonal frequency-division multiple access (OFDMA) WiMAX systems.

1 Introduction

To meet the demand of wireless access and high bandwidth transmissions, the fixed broadband wireless access (BWA) system such as the local multipoint distribution service is proposed to offer multimedia services to a number of discrete subscriber sites. The BWA system is built up by using base stations (BSs) to provide network access services for subscriber sites, which are based on the IEEE 802.16e wireless metropolitan area networks (WMANs) standards [1]. They comprise the medium access control (MAC) layer and the physical (PHY) layer [2], which dominate the main part of BWA. In IEEE 802.16e, there are many types of physical specifications such as single carrier, single carrier access, orthogonal frequency-division multiplexing (OFDM) and orthogonal frequency-division multiple

access (OFDMA) [1]. OFDM and OFDMA have the advantage of resisting interferences, providing high bandwidth and supporting diverse modulations [3–5]. In specifics the OFDMA combines two major transmission techniques: OFDM and the frequency-division multiple access (FDMA).

An OFDMA slot is based on OFDMA symbol structure, which varies within the uplink and the downlink. The structure includes the full usage of the subchannels, the partial usage of subchannels (PUSC), the distributed subcarrier permutations and the adjacent subcarrier permutation [3, 6, 7]. As IEEE 802.16e standard describes that one slot is one subchannel with two OFDMA symbols for PUSC downlink burst. OFDMA inherits inter-symbol interference (ISI) and inter-carrier interference (ICI), both

of which are against internal interference and frequency selective fading [8–10]. Therefore IEEE 802.16e WMANs standard and the digital video broadcasting return channel terrestrial proposed OFDMA for the broadband wireless multiple access systems [11–13].

However, ICI may seriously damage the orthogonal characteristic and increase the probability of ISI simultaneously [14]. These inevitable internal factors will reduce the quality of transmissions. In addition, it will also encounter unpredictable external interferences called 'noise' [15, 16], which may be caused by temperature, humidity, external electromagnetic waves and so an [17]. In the IEEE 802.16e scheduled transmission, each mobile subscriber station (MSS) has its data stream that may be arranged in a profile or in some subchannels. These profiles or subchannels are randomly put into slots for transmission, thus much transmission frame space is left empty and the profile will waste much time in transmission. These mechanisms cause serious carrier-to-interference-and-noise ratio [18]. As a result, it can be concluded that the IEEE 802.16e mechanism cannot counteract the external interference nor solve the fading problems [1]. Although the IEEE 802.16e standard is proposed to solve this difficult problem by using automatic repeat-request or hybrid automatic repeat-request retransmission mechanisms to keep a higher successful transmission probability: these mechanisms will waste a lot of system resource. Other methods such as mobility-based call admission control scheme [19] and adaptive power control [6] were also proposed to solve these problems, although these methods do not consider the arrangement of slots to enhance the transmission. Hence, their improvements were limited and might cause a lot of overheads [20, 21].

Since the error probability of a data burst depends on the channel conditions to the subscribers, the probability of successful transmission can be improved by distributing slots of each data burst into different time slots and subchannels. Therefore this paper proposes a scattered mapping method called fault-tolerant transmission mechanism (FTM) by breaking up the burst blocks into slots and then allocating them into different positions in a frame via a turntable algorithm (TA). By using FTM, the slots of all bursts in the downlink will be rearranged to support a more stable and secure transmission.

The remainder of this paper is organised as follows: Section 2 is an overview of IEEE 802.16e scheduled transmission and an illustration of our system model. Section 3 describes in detail how the FTM works to improve the fault tolerance ability in the MAC layer. Section 4 presents more proof and analysis. Section 5 describes the implementation of the proposed mechanism with simulation results. Finally, the conclusion and the future works are discussed in Section 6.

2 System model

The system model consists of multiple MSSs connecting to a centralised BS on wireless fading channels, where multiple connections (data flows) can be supported by each MSS. All connections communicate with the BS by using time division multiplexing/time division multiple access. A buffer is implemented at the BS for each connection and operates in a first-input–first-output manner. The adaptive modulation and coding (AMC) controller follows the buffer at the BS (transmitter), and the AMC selector is implemented at the MSS (receiver). Each connection employs AMC scheme at the PHY layer.

Based on OFDMA IEEE 802.16e specifications [1], the operating spectrum can be divided into N_c subchannels with each subchannel occupying N_s time slots for multiple access usage as shown in Fig. 1. In this case, the modulation scheme quadrature phase-shift keying (QPSK), M_n-ary rectangular/square quadrature amplitude modulators (QAMs), the forward error correction codes and Reed–Solomon concatenated with convolutional codes (CC) schemes are taken into consideration.

Since the wireless channel quality is mainly subject to the instantaneous signal-to-noise ratio (SNR) γ, which is the statistical description based on the general Nakagami-m model [22, 23], the received SNR γ in each frame can thus be a random variable with a gamma probability density function, that is

$$p_\gamma(\gamma) = \frac{m^m \gamma^{m-1}}{\bar{\gamma}^m \Gamma(m)} \exp\left(-\frac{m\gamma}{\bar{\gamma}}\right) \qquad (1)$$

where m is the Nakagami fading parameter ($m \geq 1/2$), $\bar{\gamma} = E\{\gamma\}$ is the average received SNR, and $\Gamma(m) = \int_0^\infty t^{m-1} e^{-t} dt$ is the gamma function [24], respectively. This channel model is suitable for flat-fading channels as well as frequency-selective fading channels in the OFDMA system. This model includes the Rayleigh channel when $m = 1$. Let N_m denote the total number of available transmission modes. According to [22], the transmission power is assumed to be constant and the
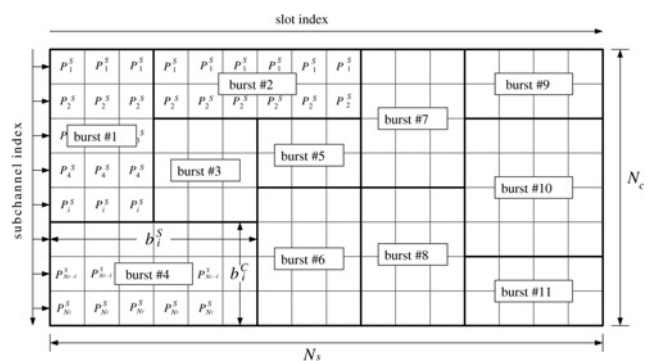
Figure 1 *Diagram of the frame structure of IEEE 802.16e*

entire SNR range is partitioned into $N_m + 1$ non-overlapping consecutive intervals, with boundary points denoted as $\{\gamma_n\}_{n=0}^{N_m+1}$. In this case, mode n is chosen when

$$\gamma \in [\gamma_n, \gamma_{n+1}), \quad n = 1, 2, \ldots, N_m \quad (2)$$

in which γ should be in the range of the corresponding modulation and coding rate. To avoid deep-channel fading, no data are sent when $\gamma_0 \leq \gamma < \gamma_1$, which corresponds to the mode $n = 0$ with rate $R_0 = 0$ bits/symbol.

To simplify the AMC design, we approximate the slot error rate (SER) expression in the additive white Gaussian noise channel as

$$\text{SER}_n(\gamma) \simeq \begin{cases} 1 & \text{if } 0 < \gamma < \gamma_p^n \\ a_n \exp(-g_n \gamma) & \text{if } \gamma \geq \gamma_p^n \end{cases} \quad (3)$$

where n is the mode index and γ is the received SNR. Parameters a_n, g_n and γ_p^n are mode dependent and are obtained by fitting (3) to the exact SER via simulations presented in [25]. Let the region boundary (switching threshold) γ_n for the transmission mode n be the minimum SNR required to guarantee S_0. Inverting the SER expression in (3), we obtain

$$\gamma_0 = 0$$
$$\gamma_n = \frac{1}{g_n} \ln\left(\frac{a_n}{S_0}\right), \quad n = 1, 2, \ldots, N_m \quad (4)$$
$$\gamma_{N+1} = +\infty$$

By using (4) to specify $\{\gamma_n\}_{n=0}^{N_m}$, one can verify that the AMC in (2) guarantees that the SER is less than or equal to S_0.

The IEEE 802.16e standard recommends that the BS has to broadcast a REP-REQ message to all MSSs periodically for channel measurements to check whether the MSS is still in the service set. Therefore the BS can obtain the SNR value by the replied REP-RSP message from each MSS to estimate the distance periodically. Let $P_i(\gamma)$ be the successful transmission probability of a time slot in the ith subchannel, where $i = 0, 1, \ldots, N_c - 1$ is the subchannel index in the frame space. The successful transmission probabilities with modulation mode n of time slots are equal if they are in the same subchannel. Then $P_i(\gamma)$ can be expressed by using (3) as

$$P_i(\gamma) \simeq \begin{cases} 0 & \text{if } 0 < \gamma < \gamma_p^n \\ 1 - a_n \exp(-g_n \gamma) & \text{if } \gamma \geq \gamma_p^n \end{cases} \quad (5)$$

Actually, the SNR value varies according to the time domain and the frequency domain. First, we assume that different subchannels, which dominate in different frequency bands, will have different SNR values and thus result in different successful transmission probabilities. Second, the SNR value varies by time in each subchannel. However, the slots are rearranged in one frame (only 5 ms as specified in the

IEEE 802.16e standard), the change of SNR value will not be significant in such a short time. Therefore we assume the SNR value of each subchannel in one frame is the same but the SNR value of each subchannel in one frame is different and follows the normal distribution. Thus, the successful transmission probability of k consecutive time slots in the ith subchannel can be simply obtained by

$$P_i(\gamma)^k = \underbrace{P_i(\gamma) P_i(\gamma) \cdots P_i(\gamma)}_{k \text{ time slots}} \quad (6)$$

Since a data burst consists of several MAC protocol data units (MPDUs) and may occupy several subchannels for data transmission, see Fig. 1, the MPDU successful probability can be expressed as $P_i(\gamma)^{N_b}$, where $N_b = L/R_n$ represents the needed number of time slots to convey the MPDU, L (bits) is the length of the MPDU and R_n is the data rate with modulation and coding mode n.

Moreover, each burst of data is constructed as a rectangular shape in the downlink as specified in the standard. Thus, a burst in one transmission frame will span several consecutive subchannels and its corresponding successful transmission probability will be

$$P_d(\gamma) = \underbrace{P_i(\gamma) \cdots P_i(\gamma)}_{s_i \text{ time slots}} \underbrace{P_{i+1}(\gamma) \cdots P_{i+1}(\gamma)}_{s_{i+1} \text{ time slots}} \cdots \quad (7)$$

where $i \in [0, N_c - 1]$ is the initial subchannel of carrying the MPDU and $N_b = s_i + s_{i+1} + \cdots + s_{i+k-1}$ for k number of subchannels. Note that $P_i(\gamma)$ may vary from subchannel to subchannel, depending on the received γ and its interferences.

Since each burst B_i consists of several MPDUs and its slot allocation should be done in rectangular basis (in the downlink period), the successful transmission probability of B_i denoted as $P_s(B_i)$ could be calculated as

$$P_s(B_i) = \prod_{j=0}^{n_m^i - 1} P_d^j(\gamma) = \prod_{j=k}^{k+n_c^i - 1} (P_j(\gamma))^{n_s^i} \quad (8)$$

where n_m^i represents the total number of MPDUs in B_i, k represents the starting subchannel of B_i, n_c^i indicates the number of subchannels and n_s^i is the number of slots in each subchannel of B_i. The frame structure of the time slot is illustrated in Fig. 2.

In the subchannel, the distribution of the probability is defined as the normal distribution. The original probability $P_s(B_i) \in [0, 1]$ can be applied to the slots in the corresponding subchannels. Under some serious interference circumstances, the specific subchannels are subject to the fading effect [22]. The model designs the adjusted
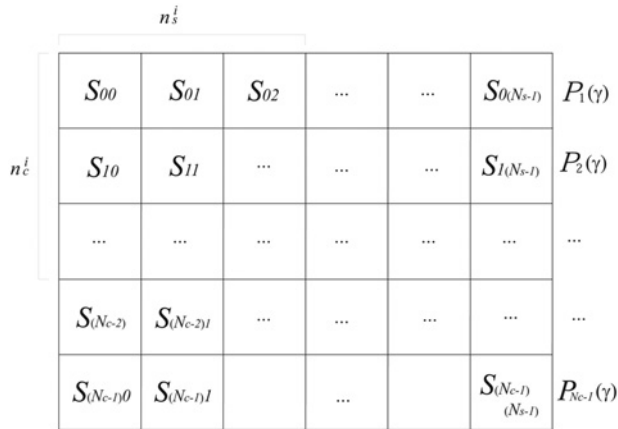
Figure 2 *Frame structure of the downlink*

probability P_i^A by

$$P_i^A = P_i(\gamma) \ (\text{mod } P_U + P_L) \tag{9}$$

where mod is the arithmetic modular operation. P_U and P_L are the adjusted successful transmission probability of the constraint upper and lower bounds, respectively.

3 Fault-tolerant transmission mechanism

3.1 Turntable algorithm

As mentioned-above, there are many burst blocks in the one frame space, each of which occupies several time slots. The $P_s(B_i)$ can be computed using the slots occupied by the burst. If each slot has its own $P_s(B_i)$ in this model, based on the previous definitions and assumptions, the probability-based scheme can modify the situation of interference on the radio channel. FTM is based on the OFDMA-PHY specification to break up the slots and distribute them into the whole frame space. This mechanism will rearrange the slots over all burst blocks. After permuting slots, we need to determine which slot is the optimal or the suboptimal solution to perform the optimal solution of the $P_s(B_i)$ in each burst. This problem is called a scattered mapping problem and is also an NP-complete mathematical permutation problem [26–28]. The main function of FTM is to increase the $P_s(B_i)$ of each burst. The higher $P_s(B_i)$, the better. This is one of the challenges for FTM.

FTM is operated by adjusting the time slot allocation of B_i with one another. The reason is that each subchannel has its corresponding successful transmission probability $P_i(\gamma)$. The probability of transmission failure caused by unpredictable external interference can be dispersed to different B_i if the subchannel is under interference. Fig. 3 shows an example of the rearranged time slots of burst blocks in the downlink frame period. This mechanism can be applied to the permutations in certain formula. Assume there are
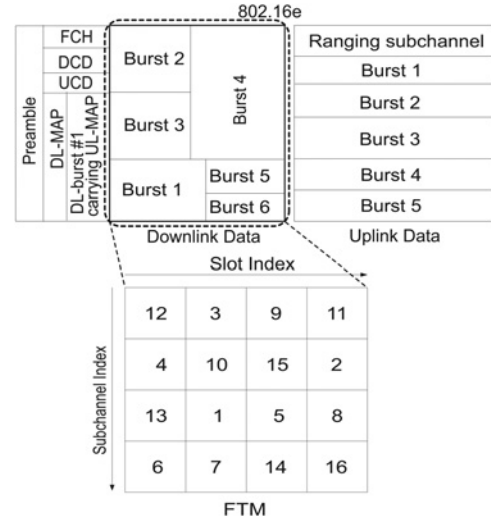
Figure 3 *Example of time slot rearrangement by FTM*

$N = N_c N_s$ time slots in the downlink subframe [29]. The permutation group G can be formulated as

$$G = \begin{pmatrix} 1 & 2 & \dots & N-1 & N \\ 13 & 20 & 5 & \dots & \dots \end{pmatrix} \tag{10}$$

where the first row indicates the order of the original permutation of the time slots and the second row indicates the new arranged permutation of original time slots. This rearrangement is a one-to-one correspondence mapping. The time $T(G)$ with the product of the permutation can be modelled as

$$T(G) = \frac{1}{|G|} \sum_{g \in G} \prod_{k=1}^{n} a_k^{j_k(g)} \tag{11}$$

where $|G|$ and $g \in G$ are the absolute time of the permutation and the time of permutation, respectively; k and $j_k(g)$ are the length of the permutation cycle and the number of cycles with the permutation cycle length k in g [30].

The detail operations of probability-based FTM are described in the following four steps.

S1. FTM calculates $P_s(B_i)$ for all $i = 0, 1, \dots, N_B - 1$, where N_B is the number of bursts in this time period by using (8).

S2. After $P_s(B_i)$ calculation, FTM determines an optimal slot allocation to all B_i by using slot rearrangement scheme. Let $P_s(t) = \sum_{i=0}^{N_B-1} P_s(B_i)/N_B$ be the average successful transmission probability of all B_i and $P_s'(t) = \sum_{i=0}^{N_B-1} P_s'(B_i)/N_B$ be the new $P_s(t)$ after rearranging slots, where $P_s'(B_i)$ is the new probability of each B_i. The problem of the determination of optimal slot allocation from G among B_i so that $P_s'(t)$ is greater than $P_s(t)$, or $P_s'(t) \geq P_s(t)$, is an NP-complete problem [30]. To obtain a better $P_s'(B_i)$,

the time slots is aligned according to their corresponding $P_i(\gamma)$ in descending order, $P(S_{ij}) \geq P(S_{kl})$ for all i, $k = 0, 1, \ldots, N_c - 1$ and j, $l = 0, 1, \ldots, N_s - 1$, where $P(S_{ij})$ denotes the successful transmission probability of each slot S_{ij}, and circle this order by letting the last slot follow the first slot as shown in Fig. 4. We note that $P(S_{ij}) = P_i(\gamma)$ since it is in the ith subchannel.

S3. Let $a_1, a_2, \ldots, a_N$ denote the aligned time slots in the turntable and $a_1 = 1, a_2 = 2, \ldots, a_N = N$. The time slot is assigned to B_i by rotating the turntable of the descending order slots. The rotational speed $V_R \in \mathbb{Z}^+$ is used to control the number of the shifts of the turntable for selecting the next slot. For example, when $V_R = 1$, B_i will select $a_1, a_2, a_3, \ldots$ or when $V_R = 3$, B_i will pick the slot index on $a_1, a_4, a_7, \ldots$, and so on if the starting slot is a_1. The selection can be achieved by using module function it follows

$$a_j = a_{j-1} + V_R \equiv 1 \,(\mathrm{mod}\, V_R) \tag{12}$$

The burst B_i with higher $P_s(B_i)$ will have the priority to select slots than the others in the turntable. The V_R will be increased by 1 when B_i finishes its selection of a_j. If the indicated a_j has been selected by other B_i, the index j will be increased by one until an unselected a_k is found. Once a_j has been selected, a_j will be removed from the turntable immediately.

S4. After scattering time slots, the $P'_s(B_i)$ of each B_i is calculated by

$$P'_s(B_i) = \prod_{j \in [0, N_c - 1]} \prod_{k \in [0, N_s - 1]} P(S_{jk}) \tag{13}$$

where S_{jk} is the selected slots by B_i.

The TA algorithm are given in Fig. 5. The following calculations illustrate the time complexity of TA. The BS sorts all slots in the frame space by the TA. There are N slots in the frame space. If sorting N slots with the sorting algorithms, the time complexity can be represented as
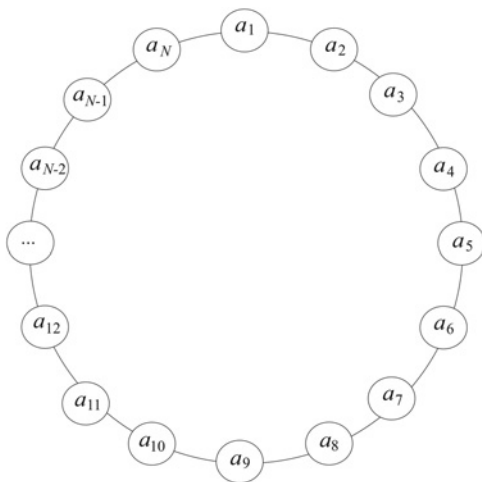
Figure 4 *Rotational diagram of turntable structure in FTM*

$N \log N = O(n \log n)$. The time loop is defined as slots picking. Hence, in the first time loop, the number of slots of a burst $|B_i|$ is much smaller than that of total slots N, in which $|B_i| \ll N$. Moreover, when the number of slots will decrease in every loop, the time complexity can be estimated as $\log_{|P_s(B_i)|} N = O(\log n)$. Accordingly, the overall time complexity of TA is evaluated as $N \log N + |P_s(B_i)| \log_{|P_s(B_i)|} N = O(n \log n)$.

3.2 FTM operations

FTM is based on the TA and operates in the MAC layer. First, FTM uses the TA to construct the downlink slot rearrangement and uses the DL-MAP message to notify MSSs for receiving their corresponding time slots in the following some frame. We note that the indicated bursts in the DL-MAP will be transmitted after several frames because each MSS needs some computational time to determine its precise slot positions after slot scrambling. The number of postponed frames can be set up by system operators as specified in the IEEE 802.16e standard [1].

The way FTM distributes the rearranged time slots information to its MSSs so that each MSS can correctly receive its corresponding slots after slot scrambling is as follows. First, both the BS and the MSS have to have the TA algorithm inside. Second, the BS will periodically broadcast the calculated $P_i(\gamma)$ based on reported SNR values from its MSSs. The SNR value can be obtained from the REP-RSP message replied by MSSs. The BS then determines an appropriate $P_i(\gamma)$ value of each subchannel to MSSs and uses the DL-MAP to notify its MSSs as specified in the IEEE 802.16e standard. The only difference is that the MSSs will use the $P_i(\gamma)$ value of each subchannel and the DL-MAP information to concurrently calculate the correct position by using the TA after receiving the DL-MAP.

There is an additional advantage in using FTM. The security and confidentiality usage of the FTM scheme is based on the slot scrambling mapping mechanism by using TA. FTM is an additional security merit in the MAC layer because any invader, which does not get permission from the BS to enter the system, will not receive the data correctly. The invaders cannot receive the correct bursts if they do not obtain a valid corresponding $P_i(\gamma)$ value of each subchannel even if they obtain the DL-MAP. On the other hand, if some invaders want to wiretap or steal information in the current BWA system by air, by probing, or by collecting the specification of BS, the invader will be able to obtain the system information but unable to handle them without the TA to calculate the mapping slot. In addition, since the slot arrangement is changed frame by frame, the scattered mapping patterns would not be duplicated. Therefore the level of security is achieved by changing the probability of all subchannels and adjusting the range of the probability value to express the whole channel quality. This way, FTM offers a higher safe transmission method.

THE TURNTABLE ALGORITHM

BEGIN

The BS sorts all slots in the frame space according to the corresponding $P(S_{ij})$ in descending order.

Take the sorted list as a set $F = \{a_1, a_2, \ldots, a_N\}$ and connect a_1 and a_N of F to be a circle.

   Repeat Roll F and pick up elements from F until all B_i are finished.

   IF $P_s(B_i) >$ others **THEN**

      Repeat Pick up $a_j, j \in \{1, 2, \ldots, N\}$ for B_i until B_i gets enough slots.

      Delete a_j from F if a_j has been chosen.

      END

   $V_R := V_R + 1$.

   END

END

Figure 5 *Turntable algorithm*

3.3 Example of slots selection

To demonstrate how TA selects burst slots to enhance $P_s(B_i)$, we illustrate an example of a downlink OFDMA channel consisting of six subchannels, each of which occupies four continuous slots as shown in Fig. 6. There are, in this example, six burst blocks arranged in a rectangle and labelled as A, B, C, D, E and F, respectively. The channel successful transmission probability of each subchannel is assumed to be various and their corresponding probabilities $P_i(\gamma)^k$, where $k = 4$ (four slots in each subchannel), are 0.5, 0.9, 0.8, 0.4, 0.7 and 0.6. The slots are labelled from left to right in each subchannel according to $P_i(\gamma)^4$ in descending order. Before rearranging the slots of each burst, FTM computes, according to (8), the $P_s(B_i)$ of each block B_i to decide the precedence of bursts. The calculated $P_s(B_i)$ is given in Table 1. Based on the priority of each $P_s(B_i)$, the sequence order of B_i will be B, C, E, F, A and D. In this example, the initial slot is $a_1 = 1$ and $V_R = 2$. These six bursts will be orderly operated by TA. The sequence of slot selection of burst B (shown with solid line arrow) is shown in Fig. 6. After the rearrangement of all slots, we can see that the $P'_s(B_i)$ given in Table 1 obtains a higher $P'_s(t)$ than that of original slot allocation to bursts, that is $P'_s(t) > P_s(t)$.
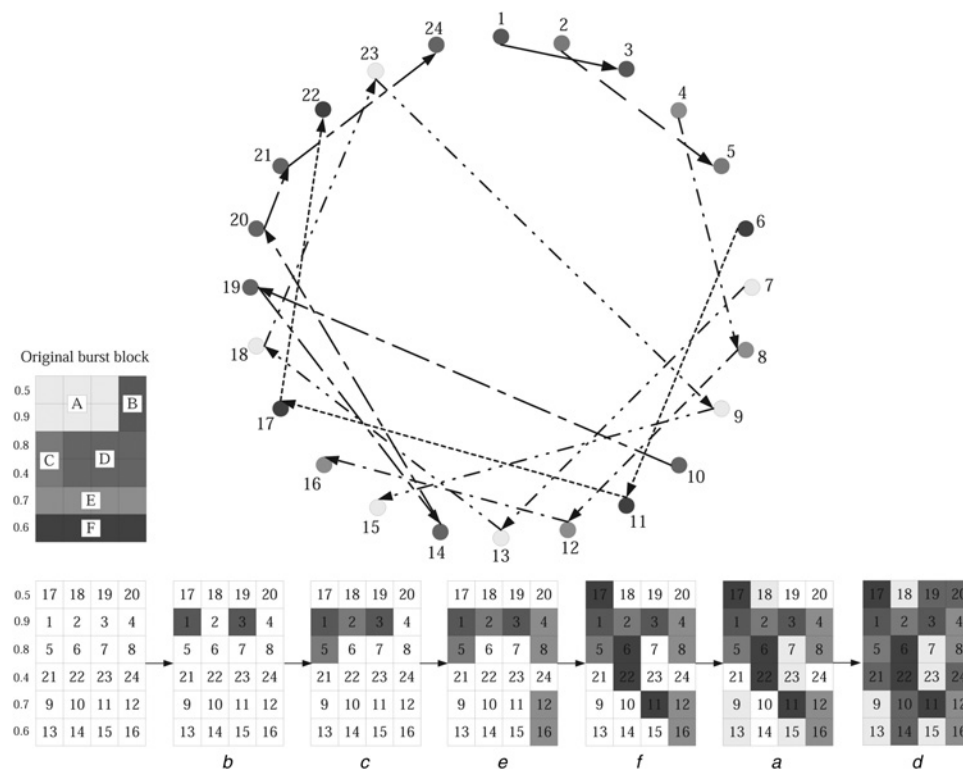
Figure 6 *Example of FTM when the initial $V_R = 2$*

Table 1 Parameter of $P_s(B_i)$

Burst block index	$P_s(B_i)$	$P_s{'}(B_i)$
A	0.091125	0.04032
B	0.45	0.81
C	0.32	0.72
D	0.032768	0.0168
E	0.2401	0.3024
F	0.1296	0.112
average probability	0.2106	0.3336

4 Proof and analysis

The goal of FTM is to allow majority users to gain greater $P_s(B_i)$ than those of the original one and the proof of this achievement is illustrated in this section. Based on the NP-complete problem, the effect and advantage of FTM are estimated as follows:

Proposition 1: The result of the FTM is proved to be better than the greedy solution (GS) in the slotted mapping problem. The GS finds the best situation during the procedure. Hence, GS is only concerned with the current situation.

Proof: Let P_i be the successful probability for each user. After P_i is processed by the FTM, the slot of P_i is

$$P_i = (S_{i1}, S_{i2}, \ldots, S_{in}) \qquad (14)$$

The successful probability of next user is P_{i+1} and $P_i \geq P_{i+1}$. Assume that there is another P_j and $P_j \geq P_i$. The P_j also has several slots as

$$P_j = (S_{j1}, S_{j2}, \ldots, S_{jn}) \qquad (15)$$

For the assumption $P_j \geq P_i$, it must have

$$\sum_{\alpha=1}^{n} P(S_{j\alpha}) \geq \sum_{\alpha=1}^{n} P(S_{i\alpha}) \qquad (16)$$

If the numbers of the slots are $S_{i1}, S_{i2}, \ldots, S_{in}, \ldots, S_{ij}$, and the probability of $S_{i(n+1)}, S_{i(n+2)}, \ldots, S_{ij}$ is greater than $S_{i1}, S_{i2}, \ldots, S_{in}$, then $P_j \geq P_i$ can be found. But in the predefinition, $\forall S_{xy}$, the slot $S_{i(n+1)}, S_{i(n+2)}, \ldots, S_{ij}$ is used by other users at the same time. In the FTM, the slot with the largest value will be regarded as the first priority slot chosen by each user. The value of second priority slot may be equal to the second or the first one. Assume there is a solution, which the total probability of its user is greater than FTM. Then, the largest value of a slot in the system must always be chosen. This is the so-called greedy solution. The calculating of GS will be faster than that of the FTM. In this solution there should be a largest slot,

which competes in the same subchannel, and it will run out earlier than the FTM. Because the largest slots run out first, it can be deduced that if $P_j > P_i$, then $P_{j+1} < P_{i+1}$. Accordingly, that $P_j \ngeq P_i$ is proved and so is the effective value P_i. □

Proposition 2: Prove that the probability of the condition of $P_s'(B_i) > P_s(B_i)$ is high.

Proof: Suppose that one user needs n slots. In the solution of IEEE 802.16e, a user can make a choice on T slots. In the solution of FTM one user can make a choice on the total frame space. Specifically, one user can make a choice on N slots, where $N > T$. Assume that the P_f is the probability of $P_s(B_i) > P_s'(B_i)$

$$P_f = \frac{\binom{T}{n}}{\binom{N}{n}} = \frac{\dfrac{T!}{n!(T-n)!}}{\dfrac{N!}{n!(N-n)!}} = \frac{T!(N-n)!}{(T-n)!N!}$$

$$= \frac{(N-n)(N-n-1)\ldots(T-n+1)}{N(N-1)\ldots(T+2)(T+1)} \qquad (17)$$

where

$$\underbrace{\frac{\overbrace{(N-n)(N-n-1)\ldots(T-n+1)}^{N-T}}{N(N-1)\ldots(T+2)(T+1)}}_{N-T} \qquad (18)$$

Because of the number of the numerator and the number of the denominator are equal. These two sequence numbers are descending, each element in each index can be compared. For example, if $N > (N-n)$, $(N-1) > (N-n-1), \ldots, (T+1) > (T-n+1)$, then the denominator is greater than the numerator in each element. Furthermore, if $N \gg T$, then it is obvious that the denominator $\gg$ the numerator. This implies that $P_f \ll 1$. Therefore that $P_s'(B_i) > P_s(B_i)$ is proved. □

5 Simulation model and results

5.1 Simulation model

To compare the performance of FTM with the legacy 802.16e mechanism, we adopt the ns-2 WiMAX simulation module [31] to evaluate the successful transmission probability and the system throughput. The TA algorithm is implemented in the MAC layer of the BS. The $P_i(\gamma)$ of subchannel i is considered as a normal distribution. The channel bandwidth is 10 MHz, which is operating in an OFDMA PHY mode with a size of 1024 fast Fourier transform (FFT) and the time division duplex mode. The frame length is 5 ms long and the ratio of downlink to uplink is 2:1. Only the downlink transmission is used in the simulation. According to the standard, in the partially used sub-carrier (PUSC) mode, there are 30

subchannels and each of them has 24 data symbols. Each slot is composed of two OFDMA symbols. Therefore the capacity of downlink $C = 30 \times 24/2 = 360$ slots.

The channel encoding scheme is the convolutional coding (CC). Different modulation schemes with coding rate, for example, QPSK 1/2, QPSK 3/4, 16-QAM 1/2, 16-QAM 3/4, 64-QAM 2/3 and 64-QAM 3/4 are considered. The usage of preamble, downlink/uplink channel descriptor (DCD/UCD), DL-MAP and UL-MAP will occupy first three OFDMA symbols, then only 270 slots are available for data transmission. Each simulation run lasts 30 s (6000 frames) and each simulation result is obtained from averaging the results from 30 independent simulation runs. The simulation model-specific parameters are listed in Table 2.

Although the channel model and fading environment will lead to a different $P_i(\gamma)$, the value of $P_i(\gamma)$ always ranges between 0 and 1. Therefore instead of investigating the channel model and fading environment, we focus on how N_B and $|B_i|$ (in slots) affect $P_s(B_i)$. This investigation will help us to realise how FTM affects $P_s(B_i)$ by comparing to legacy IEEE 802.16 transmission mechanism in the MAC layer but not in the Phy layer.

5.2 Simulation results

First, we investigate $P_s(B_i)$ with the condition $N_B \in [1, 100]$ to evaluate the performance merits between the OFDMA IEEE 802.16e transmission mechanism (denoted as 802.16e) and FTM. Fig. 7 shows the experiment results that FTM outperform 802.16e in the $P_s(B_i)$. The maximum gap of $P_s(B_i)$ between FTM and 802.16e is approximately 0.8 $(0.88 - 0.08)$ when $N_B = 1$ and a smaller gap is 0.31 $(0.53 - 0.22)$ when $N_B = 100$. As shown in Fig. 7a, the reason why the $P_s(B_i)$ of IEEE 802.16 increases but the $P_s(B_i)$ of FTM decreases when N_B

increases before $N_B = 20$, and the $P_s(B_i)$ of IEEE 802.16 still increases slightly and reaches about 0.2 when $N_B = 100$ is as follows. First, when N_B is small, it means that the size of each burst is large, for example the burst size is 648 bytes (270 slots/5*12 bytes in 16-QAM 1/2 coding rate, see Table 3) when $N_B = 5$. On the contrary, when N_B is large, for example, $N_B = 100$, the burst size is small (270 slots/100*12 bytes = 32.4 bytes). We note that these values are based on the higher modulation rate. The carried data of each burst will be smaller if the modulation rate is lower.

Based on the knowledge, when N_B is small (burst size is large), FTM (the TA algorithm) has more possibility to adjust and rearrange time slots for getting better $P_s(B_i)$. Obviously, when the N_B increases (the burst size decreases), the space (the possibility) of exchanging time slots by TA among different bursts is getting smaller. Therefore the $P_s(B_i)$ of FTM will dramatically decrease to about 0.5 (50%) when N_B reaches 20 (270 slots/20*12 bytes = 162 bytes). However, by using FTM, the $P_s(B_i)$ will remain in 0.5 and stay stably when N_B increases. Although, the $P_s(B_i)$ of IEEE 802.16e will increase slightly when N_B increases. And it will reach only 0.2 (20%) when N_B reaches 100 (32.4 byes long per each burst). We note that the value of $N_B = 100$ (concurrently 100 connections are transmitted in the WiMAX system) is not a common value in practice. In practice, the $N_B = 20-30$ is a more real value in the current WiMAX transmission system. Therefore comparing the results of Figs. 7a and b, based on the result that the $P_s(B_i)$ of the FTM still outperforms those of 802.16e and the gap between 802.16e and FTM always keeps in 30%, we can conclude that FTM is more suitable for transmission in the OFDMA-based communication system. The results can also prove that the system performance is influenced by the number of bursts. Hence, the number of bursts must be kept within a reasonably small range.

The following simulations will investigate the effect of $|B_i|$ on the WiMAX transmission system. Fig. 8 shows the relation between $P_s(B_i)$ and $|B_i|$ with a given number of slots $|B_i| \in [0, 200]$. When $|B_i| > 20$, both the $P_s(B_i)$ of 802.16e and FTM will become stable until $|B_i| = 200$. As shown in the figure, the minimum $P_s(B_i)$ of FTM will reach 0.47 when $|B_i|$ reaches 20. In addition, FTM still outperforms IEEE 802.16e by more than 30% when $|B_i| \leq 200$, owing to the effect of the appropriate slots management in the BS. The outcome of this simulation proved that $|B_i|$ should not be too large. A smaller $|B_i|$ will take less transmission time, and hence the BS can serve more users and increase the system performance; for efficiency, the burst size should be kept to no more than 20 slots and $|B_i|$ should not exceed 5% of the total frame space.

The following simulations are taken into consideration of the system throughput. The throughput indicates the valid data payload of the corresponding modulation. If the

Table 2 Simulation parameter

Parameter	Value
frame length (ms)	5
FFT size (N_{FFT})	1024
bandwidth (MHz)	10
sampling frequency (F_s) (MHz)	11.42
subcarrier spacing ($\Delta f = F_s/N_{FFT}$) (kHz)	11.16
cyclic prefix time (T_g) (µs)	11.20
useful symbol time (T_b) (µs)	89.64
OFDMA symbol time (T_s) (µs)	100.84
no. of data subcarriers in each symbol per subchannel	24
no. of subchannels for downlink data	30
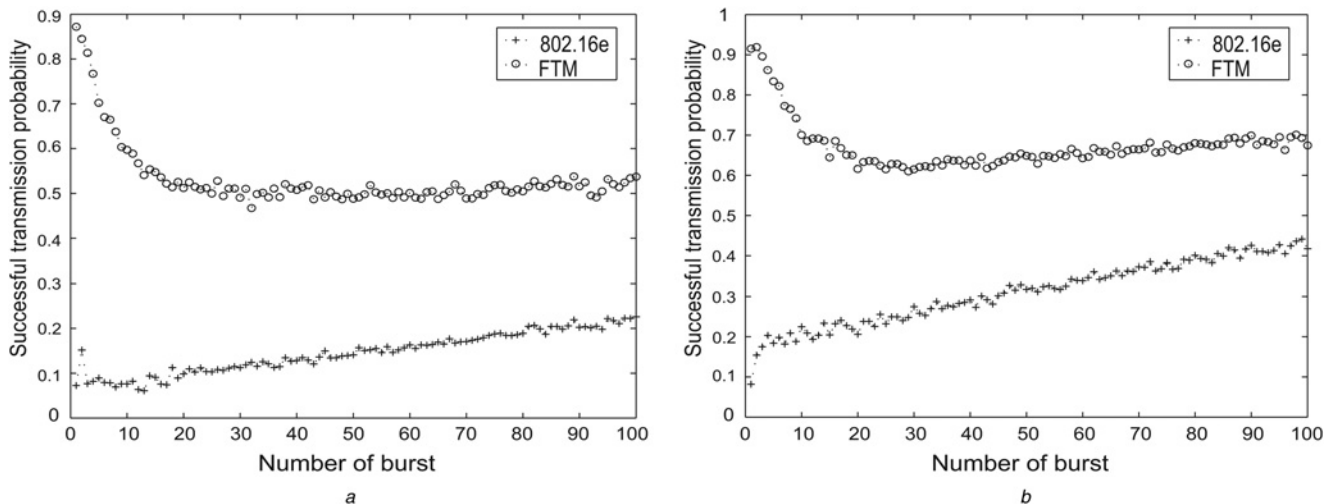
Figure 7 *Comparison of successful transmission probability derived from IEEE 802.16e and FTM against N_B in 16-QAM 1/2 modulationz*

a $P_i(\gamma) \in [0,1]$
b $P_i(\gamma) \in [0.5,1]$

number of the required transmission slots exceeds the maximum valid data payload in the assigned channels, the data will not be transmitted and its throughput will decrease. The simulation modulation parameters are listed in Table 3. Fig. 9 shows the throughput (Mbps per channel) by using 802.16e and FTM with QPSK (1/2 and 3/4), 16-QAM (1/2 and 3/4), and 64-QAM (2/3 and 3/4) modulation schemes.

In Fig. 9a with QPSK 1/2 (or Fig. 9b with QPSK 3/4), the maximum throughput of FTM reaches 4.5 Mbps (or 6.5 Mbps) and 802.16e reaches 4.4 Mbps (or 6.25 Mbps) when N_B reaches 100 and $P_i(\gamma) \in [0, 1]$. In QPSK, both the maximum throughput of the IEEE 802.16e and that of the FTM will increase with the given number of bursts. Obviously, the difference between 802.16e and FTM is within limits. It implies that QPSK is in need of the low received SNR to make slots valid. Hence, even adopting the most effective mechanism will not be a major improvement, although FTM still produces a little more throughput than IEEE 802.16e in QPSK. Moreover,

according to the results, QPSK 3/4 will need a higher received SNR than that of QPSK 1/2 to make slots valid.

Fig. 9c (or Fig. 9d) illustrate the throughput of 16-QAM 1/2 (or 3/4) modulation scheme; the maximum throughput of FTM reaches 8.8 Mbps (or 12.8 Mbps) whereas 802.16e reaches 7.8 Mbps (or 11.9 Mbps) when N_B reaches 100 and $P_i(\gamma) \in [0, 1]$. The throughput of the 16-QAM 3/4 modulation scheme is almost double the throughput of the QPSK modulation scheme. The difference between the IEEE 802.16e and FTM becomes gradually obvious. This is because 16-QAM is in need of a higher received SNR more than that of the received SNR of QPSK to make slots valid. Thus, both the throughput of the IEEE 802.16e and that of the FTM are improved more than that of the QPSK modulation scheme. FTM uses the whole slots to transmit bursts, which can always

Table 3 Modulation parameter

Modulation/coding rate	Receiver SNR (dB)	Data payload (bytes/slot)
QPSK 1/2	3.7164	6
QPSK 3/4	5.9474	9
16-QAM 1/2	9.6598	12
16-QAM 3/4	12.3610	18
64-QAM 2/3	16.6996	24
64-QAM 3/4	17.9629	27
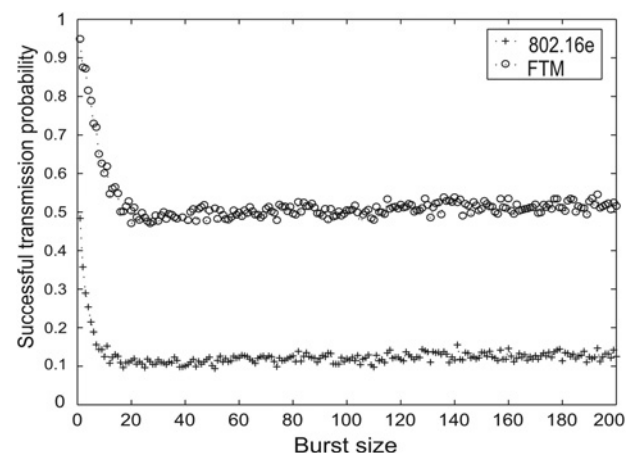
Figure 8 *Comparison of successful transmission probability derived from IEEE 802.16e and FTM against burst sizes in 16-QAM 1/2 modulation*
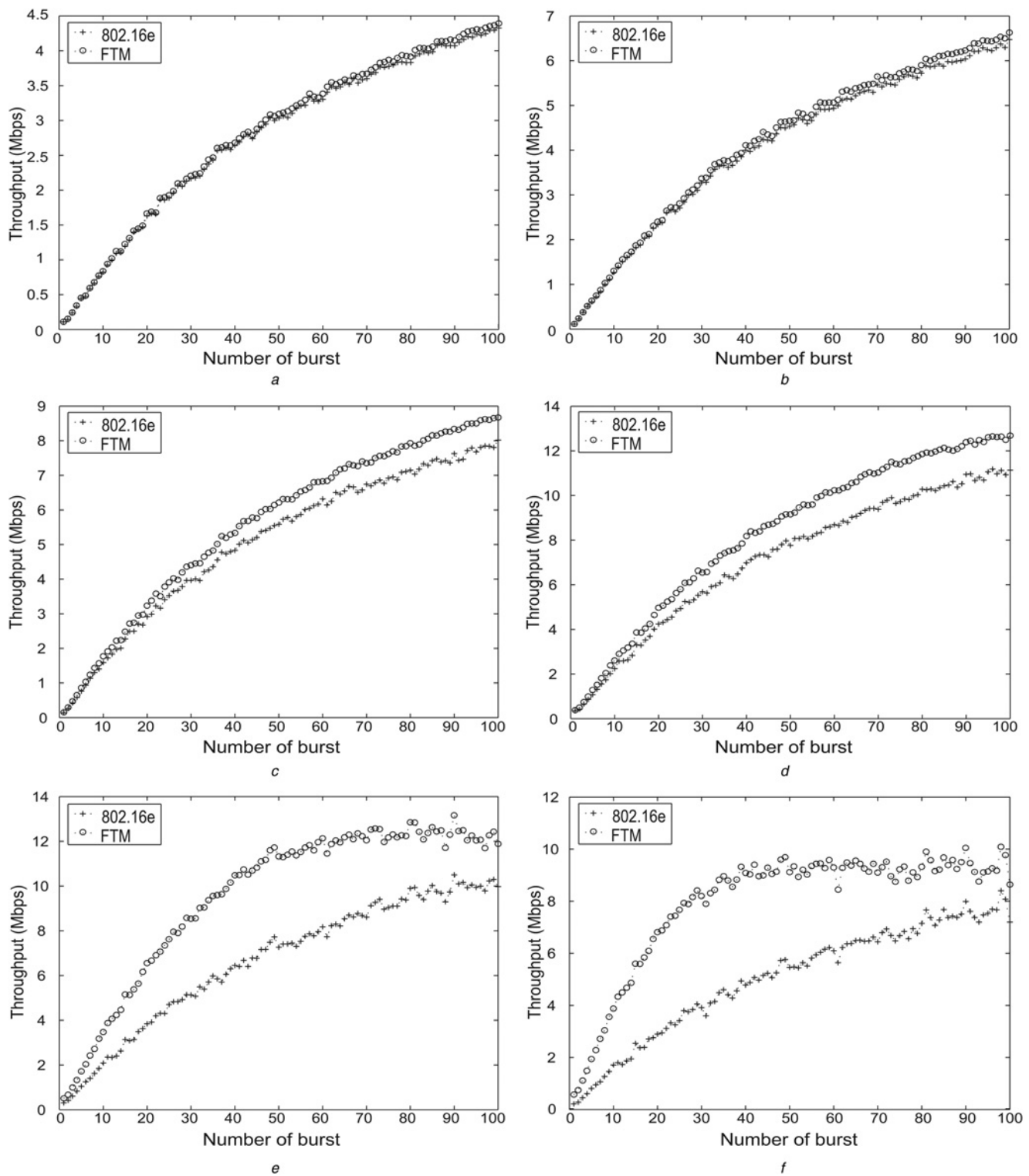
Figure 9 *Comparison of throughput derived from IEEE 802.16e and FTM against* N_B *when six different modulation scheme when* $P_i(\gamma) \in [0,1]$

a QPSK 1/2
b QPSK 3/4
c 16-QAM 1/2
d 16-QAM 3/4
e 64-QAM 2/3
f 64-QAM 3/4
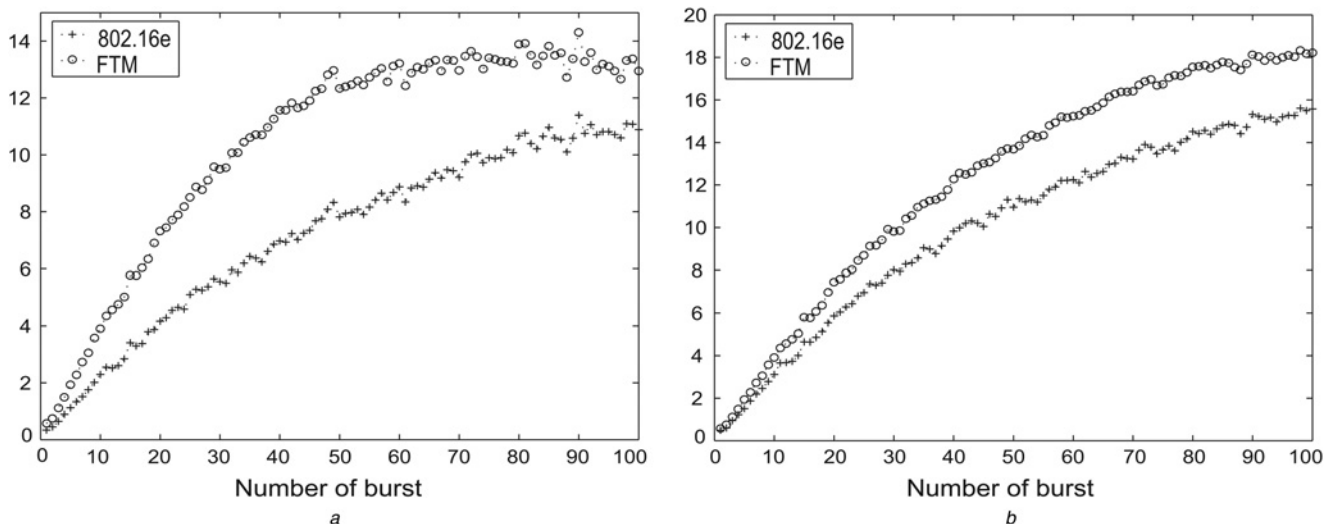
Figure 10 *Comparison of throughput derived from IEEE 802.16e and FTM against N_B with γ_n = 64-QAM 3/4*

a Channel quality $P_i(\gamma) \in [0.3, 1]$
b $P_i(\gamma) \in [0.5, 1]$

keep the highest throughput. Therefore by rearranging the frame space FTM has increased the efficiency of the bursts to transmit multiple times. Moreover, according to the results, a higher 16-QAM 3/4 modulation will lead to a higher valid data payload.

To go on with the evaluation of the high-level modulation, the throughput of 64-QAM 2/3 and 3/4 modulation schemes are shown in Figs. 9*e* and *f*. Obviously, the results are similar to those of 16-QAM modulation schemes, although the difference between the 802.16e and the FTM becomes larger. Nevertheless, as shown in 64-QAM 2/3, when $N_B = 100$ and $P_i(\gamma) \in [0, 1]$, the maximum throughput of FTM (or 802.16e) reaches 11.9 Mbps (or 9.8 Mbps) whereas in 64-QAM 3/4 the maximum throughput of FTM (or 802.16e) only reaches 9.8 Mbps (or 8.1 Mbps). The throughput of FTM in the lower 64-QAM 2/3 is higher than that of in the higher 64-QAM 3/4; the gradual curve of FTM in the lower 64-QAM 2/3 when $N_B \geq 60$ is higher than that of FTM in the higher 64-QAM 3/4 when $N_B \geq 40$. Assuming a bad channel quality, when $P_i(\gamma) \in [0, 0.3]$, the slots are not enough to serve the transmission requirement in the highest 64-QAM 3/4 modulation scheme. Therefore we will evaluate the channel quality to the influence of high-level modulation in the next simulation.

Finally, $P_i(\gamma)$ is limited to evaluate its influence under the assumption that the system has a good channel quality. Fig. 10*a* illustrates in 64-QAM 3/4, $P_i(\gamma) \in [0.3, 1]$, the maximum throughput of FTM (or 802.16e) reaches 13.1 Mbps (or 10.9 Mbps) when $N_B = 100$. We further observe that when the channel quality is raised to $P_i(\gamma) \in [0.5, 1]$, as shown in Fig. 10*b*, the maximum throughput of FTM (or 802.16e) reaches 18.1 Mbps

(or 15.5 Mbps). It is shown that the $P_s(B_i)$ of FTM still outperforms those of 802.16 in higher channel quality. In comparing Fig. 10 with Fig. 9*b*, we see the throughput has greatly increased with a given number N_B. From these results, it is concluded that a good channel quality is a necessity in high-level modulation.

Table 4 Throughput results

Modulation	Mechanism	Limited probability	Throughput (Mbps)
QPSK 1/2	IEEE 802.16e	no	4.4
	FTM	no	4.5
QPSK 3/4	IEEE 802.16e	no	6.25
	FTM	no	6.5
16-QAM 1/2	IEEE 802.16e	no	7.8
	FTM	no	8.8
16-QAM 3/4	IEEE 802.16e	no	11.9
	FTM	no	12.8
64-QAM 2/3	IEEE 802.16e	no	9.8
	FTM	no	11.9
64-QAM 3/4	IEEE 802.16e	no	8.1
	FTM	no	9.8
64-QAM 3/4	IEEE 802.16e	0.3−1	10.9
	FTM	0.3−1	13.1
64-QAM 3/4	IEEE 802.16e	0.5−1	15.5
	FTM	0.5−1	18.1

The maximum throughput of simulation results is listed in Table 4. From these results, we verify that a higher modulation will lead to a higher valid data payload and thus the transmission efficiency will be achieved. Nevertheless, a higher modulation will need a higher SNR to transmit and receive. The higher modulation will bring about higher throughput and will need better channel quality, and vice versa.

6 Conclusion

In this paper, we propose a FTM, which periodically adjusts mapping patterns for BS to control the burst size and allocate transmission slots. The simulation results illustrate that FTM can yield approximately 30% throughput and significantly raise the successful transmission probability, which outperforms IEEE 802.16e transmission mechanism. Accordingly, a conclusion can be reached that the burst size should be restricted to no more than 20 slots even under the assigned maximum burst size; a burst size should not exceed 5% of the total frame space; a higher modulation will produce larger throughput and need better channel quality and vice versa. In addition to our proposed solutions, FTM is shown as a dynamic solution that can serve all frame-based system and is ready to be disposed all over the existing network infrastructure. Hence, with transmission control in uplink, FTM can be investigated further in the future for supporting real-time QoS among macrocells.

7 Acknowledgments

8 References

[1] IEEE 802.16 Working Group: 'IEEE standard for local and metropolitan area networks – Part 16: air interface for fixed and mobile broadband wireless access systems'. IEEE Std. 802.16e-2005, February 2006

[2] YAGHOOBI H.: 'Scalable OFDMA physical layer in IEEE 802.16 wirelessMAN', *Intel Technol. J.*, 2004, **8**, (3), pp. 201–212

[3] KOFFMAN I., ROMAN V.: 'Broadband wireless access solutions based on OFDM access in IEEE 802.16', *IEEE Commun. Mag.*, 2002, **40**, (4), pp. 96–103

[4] KWON T., LEE H., CHOI S., KIM J., CHO D.H.: 'Design and implementation of a simulator based on a cross-layer protocol between MAC and PHY layers in a WiBro compatible IEEE 802.16e OFDMA system', *IEEE Commun. Mag.*, 2005, **43**, (12), pp. 136–146

[5] MINN H., BHARGAVA V.K., LETAIEF K.B.: 'A robust timing and frequency synchronization for OFDM systems', *IEEE Trans. Wirel. Commun.*, 2003, **2**, (4), pp. 822–839

[6] KULKARNI G., ADLAKHA S., SRIVASTAVA M.: 'Subcarrier allocation and bit loading algorithms for OFDMA-based wireless networks', *IEEE Trans. Mobile Comput.*, 2005, **4**, (6), pp. 652–662

[7] LAROIA R., UPPALA S., JUNYI L.: 'Designing a mobile broadband wireless access network', *IEEE Signal Proc. Mag.*, 2004, **21**, (5), pp. 20–28

[8] DIDEM K., LI G., LIU H.: 'Computationally efficient bandwidrh allocation and power control for OFDMA', *IEEE Trans. Wirel. Commun.*, 2003, **2**, (6), pp. 1150–1158

[9] JIANFENG W., THO L.N., YINGLIN X.: 'ZCZ-CDMA and OFDMA using M-QAM for broadband wireless communications', *Wirel. Commun. Mod. Comput.*, 2004, **4**, (4), pp. 427–438

[10] RENDE D., WONG T.F.: 'Bit-interleaved space-frequency coded modulation for OFDM systems', *IEEE Trans. Wirel. Commun.*, 2005, **4**, (5), pp. 2256–2266

[11] ETSI.: 'Digital video broadcasting (DVB); interaction channel for digital terrestrial television (RCT) incorporating multiple access OFDM'. Technical Report ETSI ETS, 301 958, ETSI, March 2002

[12] EKLUND C., MARKS R.B., STANWOOD K.L., WANG S.: 'IEEE standard 802.16: a technical overview of the wirelessman air interface for broadband wireless access', *IEEE Commun. Mag.*, 2002, **40**, (6), pp. 98–107

[13] YOU Y.H., JANG B.J., SONG H.K.: 'Low-complexity and MAI-robust wireless broadcasting system with return channel', *IEEE Trans. Broadcast.*, 2006, **52**, (1), pp. 71–76

[14] WILLINK T.J., WITTKE P.H., CAMPBELL L.L.: 'Evaluation of the effects of intersymbol interference in decision-feedback equalizers', *IEEE Trans. Commun.*, 2000, **48**, (4), pp. 629–636

[15] EL-SAYED M., JAFFE J.: 'A view of telecommunications network evolution', *IEEE Commun. Mag.*, 2002, **40**, (12), pp. 74–81

[16] LEE W.C.Y.: 'CS-OFDMA: a new wireless CDD physical layer scheme', *IEEE Commun. Mag.*, 2005, **43**, (2), pp. 74–79

[17] OHRTMAN F.: 'WiMax handbook-building 802.16 wireless networks' (McGrew-Hill, 2005)

[18] POLLET T., VAN BLADEL M., MOENECLAEY M.: 'BER sensitivity of OFDM systems to carrier frequency offset and wiener phase noise', *IEEE Trans. Commun.*, 1995, **43**, (234), pp. 191–193

[19] ISLAM M.M., MURSHED M.: 'Novel velocity and call duration support for QoS provision in mobile wireless networks', *IEEE Wirel. Commun.*, 2004, **11**, (5), pp. 22–30

[20] GHOSH A., WOLTER D.R., ANDREWS J.G., CHEN R.: 'Broadband wireless access with WiMax/802.16: current performance benchmarks and future potential', *IEEE Commun. Mag.*, 2005, **43**, (2), pp. 129–136

[21] LEE R., KIM J., YU J., LEE J., KIM D.: 'Capacity analysis considering channel resource overhead for mobile internet access (WiBro)'. Proc. IEEE VTC'05, Texas, May 2005, vol. 5, pp. 3082–3086

[22] ALOUINI M.S., GOLDSMITH A.J.: 'Adaptive modulation over nakagami fading channels', *Kluwer J. Wirel. Commun.*, 2000, **13**, (1/2), pp. 119–143

[23] LIU Q., WANG X., GIANNAKIS G.B.: 'A cross-layer scheduling algorithm with qos support in wireless networks', *IEEE Trans. Veh. Technol.*, 2006, **55**, (3), pp. 839–847

[24] CHEN J., TAN W.-K.: 'Predictive dynamic channel allocation scheme for improving power saving and mobility in BWA networks', *Mobile Netw. Appl.*, 2007, **12**, (1), pp. 15–30

[25] LI L., SARCA O.: 'FEC Performance with ARQ and adaptive burst profile selection', IEEE 802.16 Broadband Wireless Access Working Group, 2001, http://www.ieee802.org/16/tg3_4/contrib/80216abc-01_60.pdf

[26] BELL D.A.: 'Difficult data placement problems', *Comput. J.*, 1984, **27**, (4), pp. 315–320

[27] GAREY M.R., JOHNSON D.S.: 'Computers and intractability – a guide to the theory of NP-completeness' (Freeman, 1999)

[28] OH S.M., KIM J.H.: 'The analysis of the optimal contention period for broadband wireless access network'. Proc. IEEE PerCom 2005 Workshops, Kauai Island, Hawaii, March 2005, pp. 215–219

[29] ZHOU S., LI Y., ZHAO M., XU X., WANG J., YAO Y.: 'Novel techniques to improve downlink multiple access capacity for beyond 3G', *IEEE Commun. Mag.*, 2005, **43**, (1), pp. 61–69

[30] ROTMAN J.: 'A first course in abstract algebra' (Prentice-Hall, 1996)

[31] CHEN J., WANG C.-C., CHANG C.-W., *ET AL.*: 'The design and implementation of WiMAX module for ns-2 simulator'. Proc. ACM VALUETOOLS 2006, Pisa, Italy, October 2006, vol. 202, article 5